Int j simul model 24 (2025) 1, 29-40
Original scientific paper

SIMULATION OF ROBOTIC INSPECTIONS BASED ON SYSTEMATIC DATA ACQUISITION AND ANALYSIS

Rea, P.*; Ottaviano, E.**; Antosz, K.***; Kozlowski, E.****; Lopes, H.***** & Machado, J.*****,******
* University of Cagliari, Via Marengo, 2,09123 Cagliari (CA), Italy
** University of Cassino and Southern Lazio, via Di Biasio 43, 03043 Cassino (FR), Italy
*** Rzeszow University of Technology, al. Powstańców Warszawy 8, 35-959 Rzeszow, Poland
**** Lublin University of Technology, Nadbystrzycka 36, Lublin 20-618, Poland
***** University of Minho, Campus of Azurém, 4800-058 Guimarães, Portugal
****** Technical University of Cluj-Napoca, Muncii Ave. 103-105, 400641 Cluj-Napoca, Romania
E-Mail: pierlugi.rea@unica.it, ottaviano@unicas.it, katarzyna.antosz@prz.edu.pl, e.kozlovski@pollub.pl, d13156@dem.uminho.pt, jmachado@dem.uminho.pt

Abstract
Autonomous robots are of utmost importance across various research fields and have numerous practical applications. They can be used in scenarios such as rescue operations, security, safety management, and interventions in hazardous or hostile environments, among others. A key application of these robots is overcoming obstacles in extreme conditions, especially when human intervention is either impossible or not permitted. This paper presents modelling and simulation results based on a mathematical tool developed through systematic data acquisition and analysis, ensuring the safe operation of a robot designed to assist its pilot. The proposed predictive model is built using data collected from the robot's sensors, which are stored in a dedicated database. This data includes information on position, velocity, and acceleration, as well as their handling and processing in the presence of obstacles. The paper also includes a case study, with results that can serve as a predictive model applicable to similar conditions.
(Received in October 2024, accepted in January 2025. This paper was with the authors 2 weeks for 2 revisions.)

Key Words: Modelling, Simulation, Mobile Robots, Systematic Data Analysis, Obstacle Detection

1. INTRODUCTION

New applications for robotic systems have emerged in recent decades. Inspection, maintenance, and assessment tasks that usually required trained staff to be carried out are now performed by mobile robots in environments that are harsh for human operators. These automatic systems can perform specific operations very efficiently, avoiding dangerous risks to human operators due to the physical interaction with the surrounding environment. Several robotic inspection systems are currently utilized in industrial plants [1-3], for tunnel and mining inspection [4], in emergency search and rescue operations [5], for assessment of nuclear plants [6], military purposes [7], and space exploration [8]. The design of a mobile robot for inspection purposes should be adequate to certain terrains or locations where it is expected to operate such as in the presence of physical barriers or obstacles that it must overcome or avoid. In these complex scenarios, the teleoperation task can be increasingly difficult for the human controller since there are more actions and movements for the robot to control. Additionally, an important drawback for the operator can be caused by poor visibility. To overcome these issues, there is the possibility to automate a part or all the locomotion functions of mobile robots, thus decreasing the time spent for the mobile robot to complete its inspection function. The availability of a power source and, thus – granting autonomy – is a fundamental issue when designing an inspection robot, as it is described in [9, 10]. Regarding autonomous mobile robots, one of the main functionalities inherent to their navigation systems is the capacity to detect obstacles on their path. The information retrieved from the sensors embedded in a mobile robot is used as input data for the detection of obstacles and further processed to define the following control actions. Based on the results obtained in this stage, the response of robots can be either obstacle avoidance or overpassing. Control models, based on computer vision systems, have been applied in several fields, but they may not be fully reliable in all environments where an inspection robot may be needed, for example, when the quality of the image is degraded by poor visibility caused by low luminosity, presence of smoke, gas leakages, or dust. The focus of this work is the gathering and data treatment of internal/external sensors of a mobile robot to develop a mathematical tool, by using a systematic data analysis, able to detect obstacles and determine the right further actions and movements of a robotic system. This is very important as – with the help of a mathematical model – when the robot is remotely controlled, the operator can smoothly control it accordingly to the results, or, when the robot works autonomously, the controller can be able to consider the environmental data properly and to adapt the robot behaviour depending on specific circumstances.

This paper is divided as the following: section 2 features related works in the different areas; section 3 reports the developed mobile robot characteristics, namely its sensors and actuators. Section 4 describes the experimental tests developed for data acquisition; section 5 presents the collection and transformation of experimental data signals, as well as the developed tool, by using a systematic data analysis and the analysis of the results; and finally, in section 6, conclusions are presented and discussed.

2. RELATED WORK AND MOTIVATION

One of the possibilities to perform inspection tasks on uneven terrains is to use hybrid mobile robots. Examples of hybrid robotic systems, capable of adapting to different terrain characteristics, are given in [11-13]. Another aspect that must be considered in relation to the development of an inspection robotic system is its navigation capability. Different technologies have been used in mobile robots for inspection tasks, ranging from pure teleoperation to fully autonomous motion control. Examples of teleoperation are described in [14], while advances in predictive models and autonomous navigation are presented in [15] and [16]. In [15] a predictive model for image-based navigation was developed and tested, showing improved results despite relying solely on vision-based information. In addition, in [16] the authors studied the localisation of a mobile robot under conditions of sensor failure, highlighting the challenges of maintaining accuracy in different operational environments. A critical functionality of mobile robots that needs to be considered is obstacle detection by the robot's perception system, which gathers information about the environment and the robot's own performance [10]. In autonomous mobile robots, obstacle avoidance is a key feature of navigation systems. In an initial stage, obstacle detection is typically performed using geometric or topological maps of the environment or data collected by on-board sensors [10, 17]. Different strategies and methodologies have been developed to improve obstacle detection and navigation properties of mobile robots combining information from one [17] or multiple sensors, generally cameras and laser sensors [18]. In [17] the authors developed an algorithm based on data retrieved from a single 2D LIDAR (Light and Detection Ranging) sensor for obstacle detection and avoidance. The work [18] is an example of the implementation of different sensors data to detect and classify obstacles placed along the path of mobile robots. Recent works combining both map and map less-based approaches have been reported in [19]. Besides map-based and computer vision techniques, proximity sensors, such as infrared (IR) or sensors based on ultrasounds (US) / ultrasonics sensors, are still commonly applied in robotic systems due to their rapid response and low-cost compared with other types of sensors [20]. The work in [21] uses data obtained from five ultrasonic sensors to train an artificial neural network with the goal of determining the shape and location of objects in a mobile robot path. Data from acceleration sensors and motors power of a mobile robot were also utilized to develop a logistic regression model capable of detecting a collision between a robot and an obstacle [22].

Predictive mathematical models are increasingly being used to improve the control systems and inspection performance of mobile robots. In manufacturing, integrated inspection systems using Programmable Logic Controllers (PLCs) and Human Machine Interfaces (HMIs) have automated defect detection and feedback analysis, reducing production delays and wasted resources [23]. In the context of infrastructure inspection, innovative robotic solutions have been developed for various applications. For steel structures, a bicycle-like robot equipped with multi-sensor integration – including ultrasonic sensors and deep learning models – has been designed to navigate complex surfaces and detect rust, demonstrating its effectiveness in real-world applications [24]. The paper introduces a robotic arm developed for inspection tasks, integrating a computer vision system to enable systematic data collection and analysis [25]. In addition, the paper [26] explores the simulation of robotic inspections conducted by autonomous UAVs for power line monitoring, highlighting the use of deep learning models to ensure systematic data acquisition and analysis. Other applications of predictive mathematical models, as a tool to implement and/or improve robot's control are presented in works [27-29]. Although significant progress has been made in the development of mobile robotic inspection systems, a notable research gap remains in the integration of hybrid mobility with systematic data acquisition and predictive modelling for inspections on uneven surfaces. Existing studies focus on mechanical adaptations of hybrid robots to overcome obstacles, but often neglect advanced perception systems and real-time decision algorithms essential for dynamic environments. Current navigation and obstacle detection solutions primarily use single sensor data and static environments, limiting their effectiveness in complex inspection scenarios. There is a need for comprehensive approaches that combine hybrid mobility with multi-sensor data fusion and predictive models to improve adaptability, autonomy and inspection accuracy.

In this work, we propose a mechatronic system based on a hybrid leg-track mobile robot called THROO (Tracked Hybrid Rover to Overpass Obstacles) – intended for inspection applications. The detailed studies regarding the design and of the mobile robot is presented in [30]. The motivation of this work is to improve the inspection and monitoring in confined spaces. In the context of indoor inspection, such as in case of box girder bridges, tunnels, hollow spaces, the environmental conditions do not allow safe and reliable operation, as it is shown in Fig. 1. Furthermore, UAVs, the most common solution for outdoor areas, cannot be used due to the risk of collisions. As a result, mobile robots are typically the best option, especially when a wired connection is required, and robot control depends on visual feedback from an embedded camera. To optimize their use, it is often necessary to have additional support when visibility is poor or non-existent, due to factors such as dust, humidity, or debris. The aim of this work is to develop and validate a mathematical tool, created through systematic data analysis, that can detect obstacles based on data collected by the multiple sensors of the THROO robot. This tool provides valuable insights into the expected time for the hybrid robot to navigate an obstacle field and other performance parameters.

Figure 1: A confined space for indoor inspection: box girder bridge and detail of the cross-section.

The model can be used for predictive purposes, assisting operators in low-visibility conditions and improving robot performance during inspections in challenging environments.

This tool provides valuable insights into the expected time for the hybrid robot to navigate an obstacle field and other performance parameters. The model can be used for predictive purposes, assisting operators in low-visibility conditions and improving robot performance during inspections in challenging environments.

3. CASE STUDY – ROBOT

In this section, the main mechatronic characteristics of the THROO robot will be reported, as it will be used as hybrid mobile robot for the development of the mathematical tool.

3.1 Description of the system

The mechanical part of the THROO robot in Fig. 2 [30] has three DOFs, two of which are used for the tracks, thus giving the robot the possibility to move omnidirectionally in a plane. The main characteristics of the THROO robot are reported in Fig. 2. Its two pairs of legs, namely front and rear legs, are driven by and share an additional actuator, providing a symmetrical trajectory of the end point of the leg. The leg design is composed by a four-bar linkage with the specifications of having a support phase length b = "P_3P_1", with high h = "P_4P_2" to overpass obstacles. In general, parameters b and h depend on the given task and on the overall dimension of the robot. This design and this rather simple solution have been adopted to obtain a contemporary action of the front and rear pairs of legs and to facilitate climbing and overcoming possible obstacles.

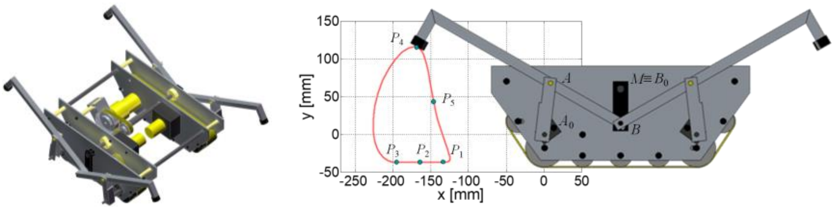

	Specifications
Length	Body: 300; body legs ext.: 550
Width	400
Height	Body: 140; body legs ext.: 200
Mass	4.5 (without batteries)
DOFs	2 (tracks) 1 (legs)

a) b)

Figure 2: Mechanical design of the THROO prototype: a) 3D view, b) trajectory of the leg endpoint.

3.2 Sensors and actuators

For the purposes of this study, the specific type of sensors (proprioceptive or exteroceptive) used is not critical; rather, it is closely related to the type of navigation and the level of sophistication required for the inspection. The overall external sensors constituting the onboard equipment for the hybrid rover suite is shown in Fig. 3.

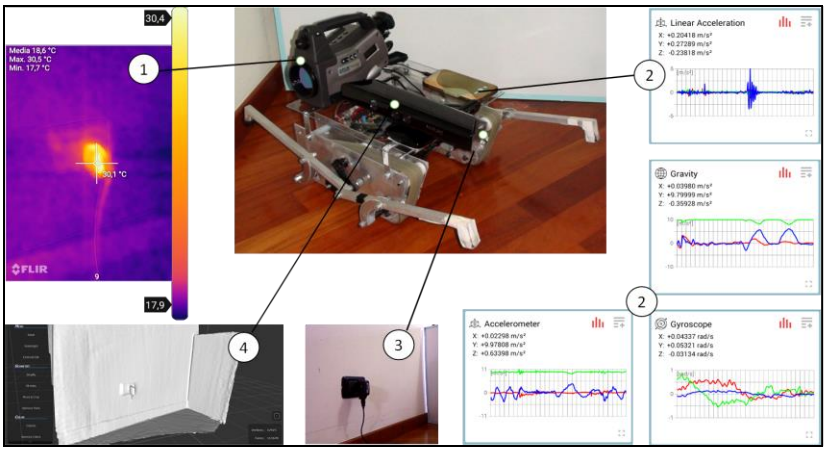

(1) the FLIR ThermaCAM S40

(2) the accelerometer, gravity and gyroscope sensors, the GPS sensor, magnetic field and acceleration sensors

(3) the front camera

(4) the Xbox Kinect 3D scan

Figure 3: A scheme of the external sensors' suite for the THROO robot and their outputs.

4. DEVELOPMENT OF THE OBSTACLE DETECTION MODEL

4.1 The goal of the developed model and the used methodology

Standardized test methods are used at the design stage to ensure that the 3D model behaves as close as possible to the real robot. Methods based on stepfield pallets [31] are effective in revealing unexpected inconsistencies between simulations and reality. In addition, a simulation method was used to analyse the data. This method has been used successfully in many studies in different fields [32, 33]. The main goal of the study was to develop a model that will allow detecting an obstacle located in the working area of the robot and that will enable us to identify a change in surface height along the robot's path. The research methodology was divided into the following steps: data collection, data pre-processing, data processing, and data post-processing. The methodology of data acquisition is shown in Fig. 4.

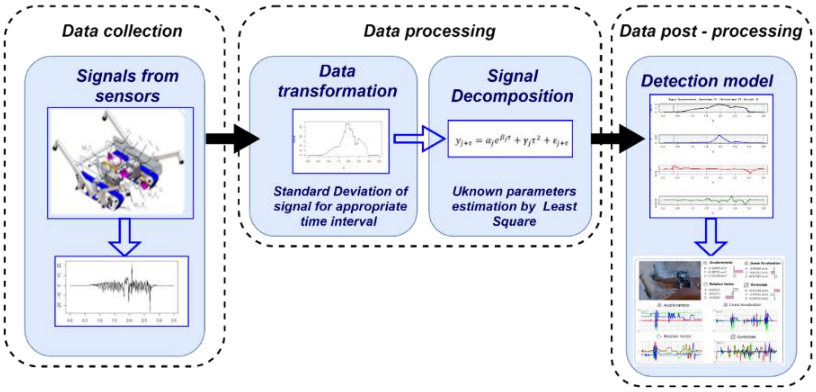

Figure 4: Methodology underling the model’s development.

4.2 Signals acquisition / data collection

Data (signals) from the sensors mounted on the robot were collected, transformed, and analysed. Signals from the accelerometers (ACC), gyroscope (G), compass (C), and rotation vector (RV) were used to develop the model. A portion of the experimental results is presented in Table I. The scheme for the stepfield pallet that was used for the experiments is displayed in Fig. 5. The signals were measured for seven different obstacle layout variants (T_1-T_7) (Fig. 6) and for three different robot velocities: V_1 = 450 mm/s, V_2 = 650 mm/s, and V_3 = 1000 mm/s. Signals from the sensors $\{(x_i, t_i)\}_{1\le i\le n}$ were read. $\{x_i\}_{1\le i\le n}$ is the sequence of the physical values, and $\{t_i\}_{1\le i\le n}$ is the sequence of moments (in ms) in which the measurements were made. Tests were carried out and the experimental results were collected. Several stepfield pallets – with a cell size of 30×30 mm – were used in several operating conditions. The tests were carried out indoor on a smooth terrain at 4 p.m. with an average temperature of $23^{\circ C}$. These signals were directly converted into a sequence of distances $\{s_i\}_{1\le i\le n}$ from the starting measurements, where $s_i = vt_i$, v – velocity, $1 \le i \le n$. In Fig. 7, the signal picked up by the accelerometer is shown.

Table I: Experiments results – sample.

SENSOR							
Time [Milliseconds]	**ACC** **Axcel**			**Time** [Milliseconds]	**RV** **Axcel**		
	X	**Y**	**Z**		**X**	**Y**	**Z**
5	-0.2003479	-0.09963989	9.72197	1	0.007594877	0.009020053	-0.9994467
…	…	…	…	…	…	…	…
104	-0.16682434	-0.17146301	9.793793	101	0.007705836	0.008959106	-0.9994381
…	…	…	…	…	…	…	…
203	-0.1716156	-0.16667175	9.784225	201	0.007661813	0.008961996	-0.9994417

The set of considered times is at 5, 13, 24, 33, 43, 54, 63, 73, 83, 94, 104, 113, 124, 133, 143, 153, 164, 173, 183, 193, 203 milliseconds and an illustration are presented in this figure. Fig. 7 shows the raw accelerometer signal, as the starting point for the analysis.

0	0	0	0	1	1	0	0	0	1	1	0	0	0	1	1	0	0	0	0
0	0	0	0	1	1	0	0	0	1	1	0	0	0	1	1	0	0	0	0
0	0	0	0	1	1	0	0	0	1	1	0	0	0	1	1	0	0	0	0
0	0	0	0	1	1	0	0	0	1	1	0	0	0	1	1	0	0	0	0
0	0	0	0	1	1	0	0	0	1	1	0	0	0	1	1	0	0	0	0
0	0	0	0	1	1	0	0	0	1	1	0	0	0	1	1	0	0	0	0
0	0	0	0	1	1	0	0	0	1	1	0	0	0	1	1	0	0	0	0
0	0	0	0	1	1	0	0	0	1	1	0	0	0	1	1	0	0	0	0
0	0	0	0	1	1	0	0	0	1	1	0	0	0	1	1	0	0	0	0
0	0	0	0	1	1	0	0	0	1	1	0	0	0	1	1	0	0	0	0

Figure 5: Example of the field used for testing the hybrid rover.

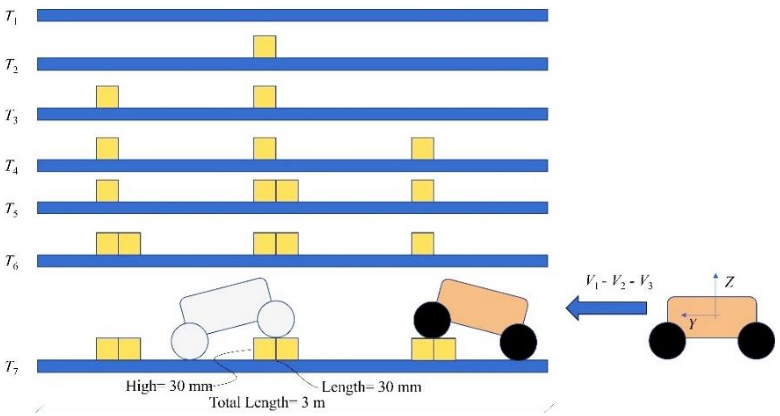

Figure 6: Graphic presentation of the experiment.

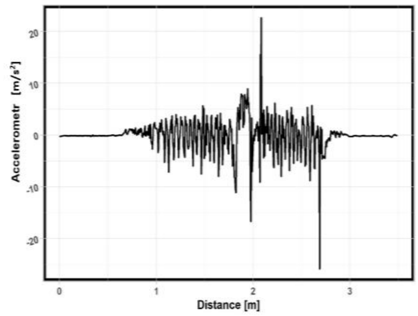

Figure 7: Raw signal registered by the accelerometer – example.

4.3 Data transformation

The first step of data pre-processing was data transformation [34, 35]. The standard deviation of signal for an appropriate time interval was used. For the sequence values $\{x_i\}_{1\le i\le n}$, where for a set $m \in N$ of every subsequence $\{x_{max(1,i-m)}, x_{max(1,i-m)+1}, \dots, x_{min(i+m,n)}\}_{1\le i\le n}$ the value of the standard deviation estimator was determined, and the sequence $\{y_i\}_{1\le i\le n}$ was received:

$$y_i = \frac{1}{min(i+m,n)+1-max(1,i-m)} \sum_{j=max(1,i-m)}^{min(i+m,n)} \left(x_j - \bar{x}_j\right)^2 \quad (1)$$

$$\bar{x}_j = \frac{1}{min(i+m,n)+1-max(1,i-m)} \sum_{j=max(1,i-m)}^{min(i+m,n)} x_j \quad (2)$$

for $1 \le i \le n$.

To determine when the obstacle occurs and the time of complete stabilization of the robot for a set k, first the behaviour of each sequence $\{y_{j+\tau}\}_{-min(j-1,k)\le\tau\le min(k,n-j)}$ was modelled:

$$y_{j+\tau} = \alpha_j e^{\beta_j \tau} + \gamma_j \tau^2 + \varepsilon_{j+\tau}, \quad (3)$$

where ε_j is a normally distributed random variable $N(0,\sigma^2)$. For a set j the value of the estimators $\alpha_j, \beta_j, \gamma_j$ using the Least Squares Method were determined. Indeed, to solve the task:

$$\min_{\alpha_j,\beta_j,\gamma_j} \sum_{\tau=-min(j-1,k)}^{min(k,n-j)} \left(y_{j+\tau} - \alpha_j e^{\beta_j \tau} - \gamma_j \tau^2\right)^2 \quad (4)$$

In Fig. 8, the signal (example) after pre-processing is presented.

Estimator sequences $\{\alpha_i\}_{1\le i\le n}$, $\{\beta_i\}_{1\le i\le n}$, $\{\gamma_i\}_{1\le i\le n}$ represent, respectively:

- the level of variation of the raw signal picked up by the sensor;
- an increase (in the case of $\beta_j > 0$) or a decrease (in the case of $\beta_j < 0$) of the variation in the signal from the sensor.

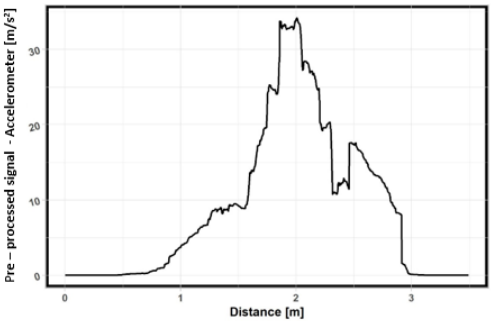

Figure 8: Signal after pre-processing – example.

To identify the presence of the obstacle (vibration increase) or the robot stabilization moments (vibration decrease), the behaviour of the sequence $\{\beta_i\}_{1\le i\le n}$ is observed to determine the local peaks. The local maximum means an increase in vibrations (the moment of emergence of an obstacle), while the local minimum means a decrease in vibration (stabilization of the robot). The local maximum of the sequence $\{\gamma_i\}_{1\le i\le n}$ shows the instant with the highest intensity of vibrations. In Figs. 9 to 14, an example of the processed signal $\{y_i\}_{1\le i\le n}$. decomposition is presented. The processed signal $\{y_i\}_{1\le i\le n}$ in the upper left corner of figures is presented. This signal was decomposed into the sequences of parameters: $\{\alpha_i\}_{1\le i\le n}$, $\{\beta_i\}_{1\le i\le n}$, $\{\gamma_i\}_{1\le i\le n}$. The signals were collected by sensors, at different speeds of the robot, for several obstacles positioned in planes X, Y and Z. Figs. 9 to 14 present different scenarios for a moving robot: with different sensors (gravity, compass, accelerometer; different speeds of robot (V_1, V_2, V_3); and different axes (X, Y, Z). The plots allow the analysis of the change in the signal value and its decomposition parameters. Analysis of the change in the value of the α_j estimator allows the identification of the moment of occurrence of the change in the height of the surface of the robot's path (blue vertical line). The increasing value of the α_j estimator means the emergence of an obstacle. The analysis of the value of the β_j estimator allows the identification of the rapid increase or decrease of the signal value. The red vertical line in the graphs of the β_j estimator means the maximum peak (the maximum value of the parameter). Changes in the value of the γ_j estimator represent changes in the values of the signal curve (parabola). The smallest values of the γ_j estimator mean a quick temporary increase of the signal value, and then a temporary decrease of its value. The analysis of the signal decomposition shows that the developed model is effective in detecting an obstacle (analyses of the $\alpha_j$estimator – blue vertical line), regardless of the signal recorded by the t sensors, the speeds of the robot, the variants of obstacles position.

Fig. 9 shows the signal registered for gravity, with the velocity V_1 = 450 mm/s, and for the obstacle type T_2 (Fig. 6) on the X-axis. Analysing in this scenario the series for $\{\alpha_i\}_{1\le i\le n}$, $\{\beta_i\}_{1\le i\le n}$, their value changes significantly after distance s = 0.35 and s = 1.5. The first change is responsible for approaching the palette. The second one means the presence of an obstacle. Fig. 10 shows the signal registered for gravity, with the velocity V_1 = 650 mm/s, for the obstacle type T_2 (Fig. 6) positioned on the X-axis. The same as in the case of Fig. 9, from time series realization $\{\alpha_i\}_{1\le i\le n}$, $\{\beta_i\}_{1\le i\le n}$ we can conclude that the value of the series are significantly changing over the distance s = 0.5 and s = 1.8. The first change is responsible once more for approaching the palette. The second means the presence of an obstacle. At the value of s = 3.2, the moment of overcoming the obstacle can be observed (the values of the series $\{\alpha_i\}_{1\leq i\leq n}$, $\{\beta_i\}_{1\leq i\leq n}$ decrease significantly again).

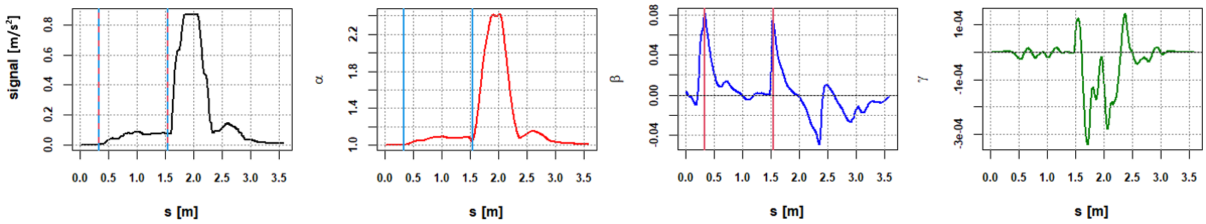

Figure 9: Gravity signal decomposition for the robot velocity V_1 and obstacle type: T_2 in X-axis.

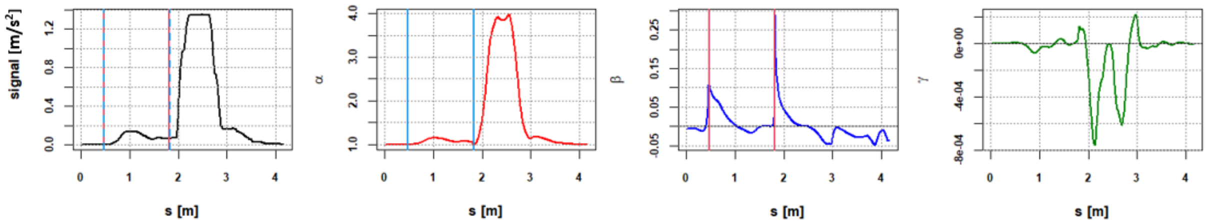

Figure 10: Gravity signal decomposition for the robot velocity V_2 and obstacle type: T_2 in X-axis.

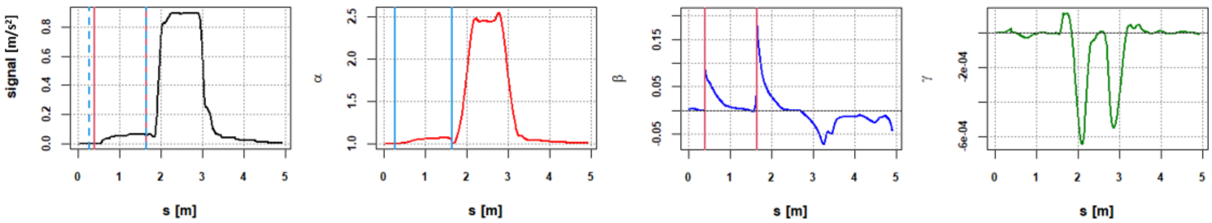

Figure 11: Gravity signal decomposition for the robot velocity V_3 and obstacle type: T_2 in X-axis.

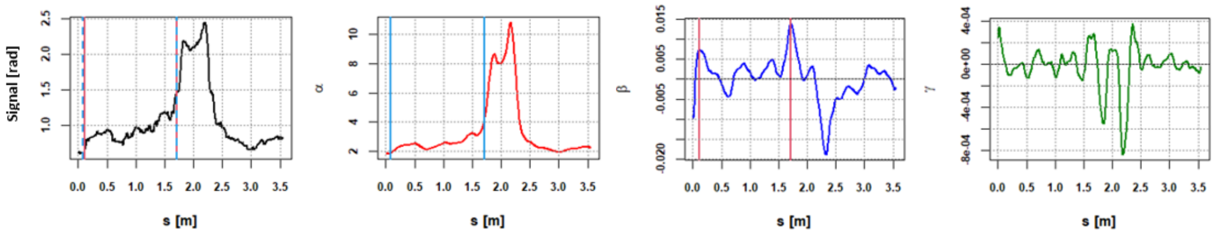

Figure 12: Compass signal decomposition for the robot velocity V_1 and obstacle type: T_2 in Y-axis.

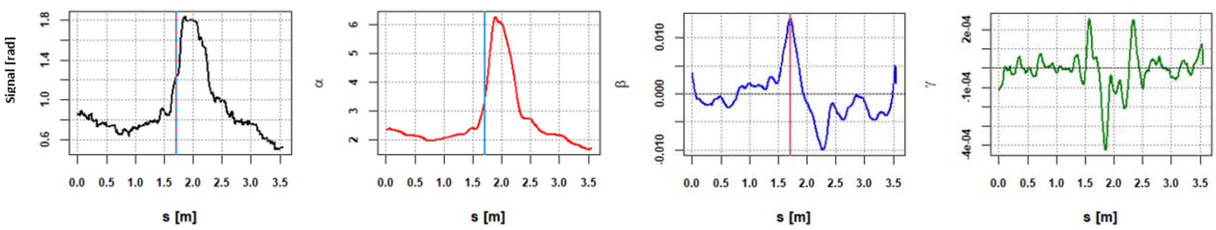

Figure 13: Compass signal decomposition for the robot velocity V_1 and obstacle type: T_2 in Z-axis.

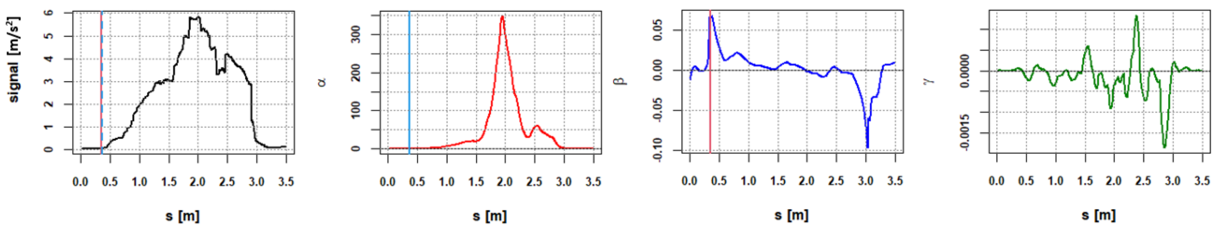

Figure 14: Accelerometer signal decomposition for the robot velocity V_1 and obstacle type: T_2 in X-axis.

Fig. 11 shows the signal registered for gravity, with a velocity V_1 = 1000 mm/s, for the obstacle type T_2 (Fig. 6) positioned on the Y-axis. In this scenario, a significant change in the series $\{\alpha_i\}_{1\le i\le n}$, $\{\beta_i\}_{1\le i\le n}$ is noticeable at the distance s = 1.8 to s = 3.2. At this distance, the position of the robot is changing. Fig. 12 shows the signal registered by the compass, with the velocity V_1 = 450 mm/s, for the obstacle type T_2 (Fig. 6) positioned on the Y-axis. In this scenario, a significant change in the series $\{\alpha_i\}_{1\le i\le n}$, $\{\beta_i\}_{1\le i\le n}$ is noticeable, one more time, at the distance range s = 1.5 to s = 2.5. Fig. 13 presents the signal registered by the compass, with a velocity V_1 = 450 mm/s, for the obstacle type T_2 (Fig. 6) positioned on the Z-axis. In this scenario the moment changing the position of the robot can observed the distance range s = 1.5 to s = 2.5 (a significant change in the series $\{\alpha_i\}_{1\le i\le n}$, $\{\beta_i\}_{1\le i\le n}$ is noticeable). Fig. 14 shows the signal of the accelerometer, with a velocity V_1 = 450 mm/s, for the obstacle type T_2 (Fig. 6) on the X-axis. Analysing – in this scenario – the series especially for $\{\alpha_i\}_{1\le i\le n}$, $\{\beta_i\}_{1\le i\le n}$, we can observe that their value changes significantly after the distance s = 1.5.

In summary, the results presented in Figs. 9 to 14 demonstrate that the developed model effectively identifies moments when the robot's position changes and when obstacles appear in its path. This model can be integrated into the robot's measurement system, enabling real-time analysis of the signals collected by the sensors (Fig. 15). The signal collection frequency is based on a fixed number of currently analysed measurements. Moreover, the changing of the signal decomposition and the value of the estimators $\alpha_j, \beta_j, \gamma_j$ can be also observed and analysed by the operator with a similar display as the one depicted in Fig. 14.

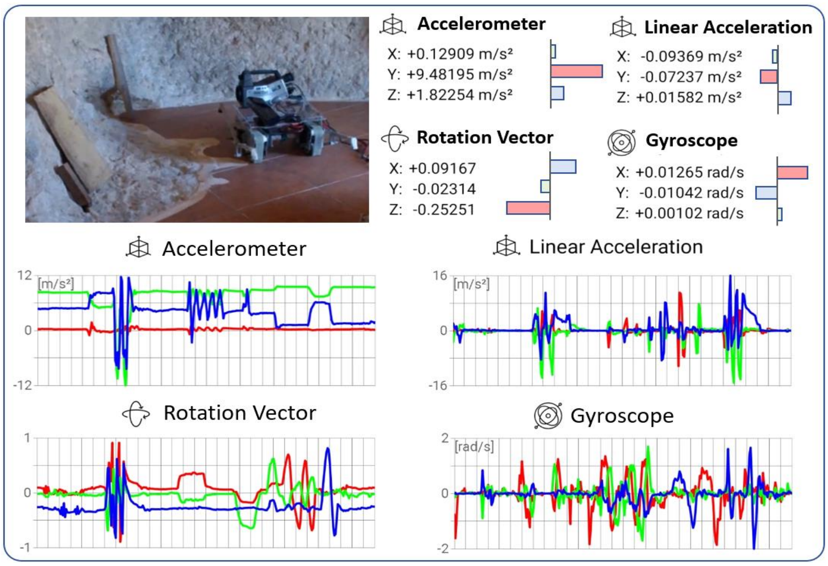

Figure 15: Visualization of the values picked up by the sensors.

5. CONCLUSIONS

Mobile robots are increasingly being used to assist or replace personnel in the inspection of various structures and infrastructures. In the case of indoor inspections such as in confined spaces like boxed girder bridges environmental conditions often prevent safe and reliable operation by human staff, while UAVs cannot be used due to collision risks. As a result, mobile robots are typically the best option, especially since they often require a wired connection, and their control relies on visual feedback provided by an embedded camera. To optimize their use, it is often beneficial to have additional support in situations with poor or no visibility. This paper presents a predictive model developed using data collected by the robot's sensors, which is stored in a database. The primary aim of this model is to enhance the robot's performance, whether under teleoperation by a pilot or through autonomous control by the robot’s algorithm, to ensure the success of the operation. In this paper, we proposed a novel approach that offers a new solution not yet explored in the literature. We have identified the processed signal $\{y_i\}_{1\le i\le n}$ for each subsequence using model (3) by solving task (4), thus determining estimators of $\{\alpha_i\}_{1\le i\le n}$, $\{\beta_i\}_{1\le i\le n}$, $\{\gamma_i\}_{1\le i\le n}$ parameters for this subsequence, while creating sequences for these parameters. Changing the values of these parameters has allowed for an accurate identification of the obstacle encountered by the robot along its path, as shown in our demonstration. The primary objective of this research was not to analyse the signal as a time series using classical methods such as wavelet analysis or spectral analysis, but to decompose the signal into components with a linear input to the model. By analysing these components, it was demonstrated that a simple model can be implemented to detect obstacles without requiring the robot's actual position. While many scientific studies develop predictive models based on a training set, the proposed approach does not use a training set. Instead, model parameters are estimated in real time, with time series containing structural parameters analysed on-line. The proposed mathematical tool successfully detected all obstacles with a location error of less than 0.15 m. Due to its effectiveness, this model can be applied to any robot operating conditions, particularly in situations with poor visibility, and in the absence of a GPS signal, 3D scans, or LiDAR. The method and approach we have used can be adopted for any mobile robot operating in challenging scenarios, where different types of obstacles and sensor data are handled using a similar methodology.

ACKNOWLEDGEMENTS

This work was supported by the project "New frontiers in adaptive modular robotics for patient-centered medical rehabilitation – ASKLEPIOS", funded by the European Union – NextGenerationEU and the Romanian Government, under the National Recovery and Resilience Plan for Romania, contract no. 760071/23.05.2023, code CF 121/15.11.2022, with the Romanian Ministry of Research, Innovation, and Digitalization, within Component 9, investment I8; and by Fundação para a Ciência e Tecnologia (FCT) within the RD Units Project Scope: UIDP/04077/2020 and UIDB/04077/2020.

REFERENCES

[1] Maurtua, I.; Susperregi, L.; Fernández, A.; Tubío, C.; Perez, C.; Rodríguez, J.; Felsch, T.; Ghrissi, M. (2014). MAINBOT – mobile robots for inspection and maintenance in extensive industrial plants, *Energy Procedia*, Vol. 49, 1810-1819, doi:10.1016/j.egypro.2014.03.192

[2] JettyRobot. Robotic Work in Pipes Around the World, from *https://www.jettyrobot.com/*, accessed on 01-06-2024

[3] Rea, P.; Ottaviano, E.; Castillo-Garcia, F. J.; Gonzalez-Rodriguez, A. (2022). Inspection robotic system: design and simulation for indoor and outdoor surveys, Machado, J.; Soares, F.; Trojanowska, J.; Yildirim, S. (Eds.), *Innovations in Mechatronics Engineering, Lecture Notes in Mechanical Engineering*, Springer, Cham, 313-321, doi:10.1007/978-3-030-79168-1_29

[4] Szrek, J.; Wodecki, J.; Błażej, R.; Zimroz, R. (2020). An inspection robot for belt conveyor maintenance in underground mine – infrared thermography for overheated idlers detection, *Applied Sciences*, Vol. 10, No. 14, Paper 4984, 17 pages, doi:10.3390/app10144984

[5] Murphy, R. R.; Tadokoro, S.; Nardi, D.; Jacoff, A.; Fiorini, P.; Choset, H.; Erkmen, A. M. (2008). Search and rescue robotics, Siciliano, B.; Khatib, O. (Eds.), *Springer Handbook of Robotics*, Springer, Berlin, 1151-1173, doi:10.1007/978-3-540-30301-5_51

[6] Rohmer, E.; Yoshida, T.; Ohno, K.; Nagatani, K.; Tadokoro, S.; Konayagi, E. (2010). Quince : a collaborative mobile robotic platform for rescue robots research and development, *The Abstracts of the International Conference on Advanced Mechatronics: Toward Evolutionary Fusion of IT and Mechatronics (ICAM)*, Vol. 2010.5, 225-230, doi:10.1299/jsmeicam.2010.5.225

[7] Szegedi, P.; Koronváry, P.; Békési, B. (2017). The use of robots in military operations, *Scientific Research and Education in the Air Force – AFASES 2017 Proceedings (Aerial Systems and Aerospace Engineering)*, 221-230, doi:10.19062/2247-3173.2017.19.1.25

[8] Seriani, S. (2019). A new mechanism for soft landing in robotic space exploration, *Robotics*, Vol. 8, No. 4, Paper 103, 22 pages, doi:10.3390/robotics8040103
[9] Kala, R. (2023). *Autonomous Mobile Robots: Planning, Navigation and Simulation*, Elsevier, Imprint Academic Press, Cambridge, doi:10.1016/C2022-0-00636-X
[10] Rubio, F.; Valero, F.; Llopis-Albert, C. (2019). A review of mobile robots: concepts, methods, theoretical framework, and applications, *International Journal of Advanced Robotic Systems*, Vol. 16, No. 2, 22 pages, doi:10.1177/1729881419839596
[11] Kim, Y.-G.; Kwak, J.-H.; Hong, D.-H.; Kim, I.-H.; Shin, D.-H.; An, J. (2012). Autonomous terrain adaptation and user-friendly tele-operation of wheel-track hybrid mobile robot, *International Journal of Precision Engineering and Manufacturing*, Vol. 13, No. 10, 1781-1788, doi:10.1007/s12541-012-0234-9
[12] Seo, B.; Kim, H.; Kim, M.; Jeong, K.; Seo, T. (2013). FlipBot: a new field robotic platform for fast stair climbing, *International Journal of Precision Engineering and Manufacturing*, Vol. 14, No. 11, 1909-1914, doi:10.1007/s12541-013-0259-8
[13] De Luca, A.; Muratore, L.; Raghavan, V. S.; Antonucci, D.; Tsagarakis, N. G. (2021). Autonomous obstacle crossing strategies for the hybrid wheeled-legged robot Centauro, *Frontiers in Robotics and AI*, Vol. 8, Paper 721001, 16 pages, doi:10.3389/frobt.2021.721001
[14] Becerra, H. M.; Sagüés, C.; Mezouar, Y.; Hayet, J.-B. (2014). Visual navigation of wheeled mobile robots using direct feedback of a geometric constraint, *Autonomous Robots*, Vol. 37, 137-156, doi:10.1007/s10514-014-9382-3
[15] Vecchio, G.; Palazzo, S.; Guastella, D. C.; Giordano, D.; Muscato, G.; Spampinato, C. (2024). Terrain traversability prediction through self-supervised learning and unsupervised domain adaptation on synthetic data, *Autonomous Robots*, Vol. 48, Paper 4, 19 pages, doi:10.1007/s10514-024-10158-4
[16] Kheirandish, M.; Yazdi, E. A.; Mohammadi, H.; Mohammadi, M. (2023). A fault-tolerant sensor fusion in mobile robots using multiple model Kalman filters, *Robotics and Autonomous Systems*, Vol. 161, Paper 104343, 24 pages, doi:10.1016/j.robot.2022.104343
[17] Peng, Y.; Qu, D.; Zhong, Y.; Xie, S.; Luo, J.; Gu, J. (2015). The obstacle detection and obstacle avoidance algorithm based on 2-D lidar, *2015 IEEE International Conference on Information and Automation*, 1648-1653, doi:10.1109/ICInfA.2015.7279550
[18] Yuan, W.; Li, Z.; Su, C.-Y. (2021). Multisensor-based navigation and control of a mobile service robot, *IEEE Transactions on Systems, Man, and Cybernetics: Systems*, Vol. 51, No. 4, 2624-2634, doi:10.1109/TSMC.2019.2916932
[19] Li, J.; Qin, H.; Wang, J.; Li, J. (2022). OpenStreetMap-based autonomous navigation for the four wheel-legged robot via 3D-Lidar and CCD camera, *IEEE Transactions on Industrial Electronics*, Vol. 69, No. 3, 2708-2717, doi:10.1109/TIE.2021.3070508
[20] Farias, G.; Fabregas, E.; Peralta, E.; Vargas, H.; Hermosilla, G.; Garcia, G.; Dormido, S. (2018). A neural network approach for building an obstacle detection model by fusion of proximity sensors data, *Sensors*, Vol. 18, No. 3, Paper 683, 18 pages, doi:10.3390/s18030683
[21] De Simone, M. C.; Rivera, Z. B.; Guida, D. (2018). Obstacle avoidance system for unmanned ground vehicles by using ultrasonic sensors, *Machines*, Vol. 6, No. 2, Paper 18, 13 pages, doi:10.3390/machines6020018
[22] Becker, F.; Ebner, M. (2019). Collision detection for a mobile robot using logistic regression, *Proceedings of the 16th International Conference on Informatics in Control, Automation and Robotics (ICINCO 2019)*, Vol. 2, 167-173, doi:10.5220/0007768601670173
[23] Mikhail, M.; Abad, K. (2023). Robotic inspection and automated analysis system for advanced manufacturing, *IAES International Journal of Robotics and Automation (IJRA)*, Vol. 12, No. 4, 352-364, doi:10.11591/ijra.v12i4.pp352-364
[24] Nguyen, S. T.; La, K. T.; La, H. M. (2024). Agile robotic inspection of steel structures: a bicycle-like approach with multisensor integration, *Journal of Field Robotics*, Vol. 41, No. 2, 396-419, doi:10.1002/rob.22266
[25] Alnowaini, G.; Alttal, A.; Alhaj, A. (2021). Design and simulation robotic arm with computer vision for inspection process, *2021 International Conference of Technology, Science and Administration (ICTSA)*, 6 pages, doi:10.1109/ICTSA52017.2021.9406541

[26] Zaidi, M. A.; Tariq, F. (2023). Revolutionizing power line inspection: automated data acquisition through autonomous UAVs in simulated environment, *South Florida Journal of Development*, Vol. 4, No. 3, 1199-1215, doi:10.46932/sfjdv4n3-014

[27] Carron, A.; Arcari, E.; Wermelinger, M.; Hewing, L.; Hutter, M.; Zeilinger, M. N. (2019). Data-driven model predictive control for trajectory tracking with a robotic arm, *IEEE Robotics and Automation Letters*, Vol. 4, No. 4, 3758-3765, doi:10.1109/LRA.2019.2929987

[28] Kang, E.; Qiao, H.; Gao, J.; Yang, W. (2021). Neural network-based model predictive tracking control of an uncertain robotic manipulator with input constraints, *ISA Transactions*, Vol. 109, 89-101, doi:10.1016/j.isatra.2020.10.009

[29] Wane, S. A.; Butler, M.; Bautista, A. J. (2024). Development of a microcontroller based robot and its use in teaching control and navigation, *Proceedings on Engineering Sciences*, Vol. 6, No. 4, 1685-1694, doi:10.24874/PES06.04.027

[30] Ottaviano, E.; Rea, P.; Castelli, G. (2014). THROO: a Tracked Hybrid Rover to Overpass Obstacles, *Advanced Robotics*, Vol. 28, No. 10, 683-694, doi:10.1080/01691864.2014.891949

[31] Jacoff, A.; Downs, A.; Virts, A.; Messina, E. (2008). Stepfield pallets: repeatable terrain for evaluating robot mobility, *Proceedings of the 8th Workshop on Performance Metrics for Intelligent Systems (PerMIS'08)*, 29-34, doi:10.1145/1774674.1774680

[32] Budiraharjo, R.; Sarno, R.; Wijaya, D. R.; Prasetyo, H. N.; Waspada, I. (2024). Simulations to predict process model alignment with standard operating procedure, *International Journal of Simulation Modelling*, Vol. 23, No. 1, 17-28, doi:10.2507/IJSIMM23-1-657

[33] Chai, G. F.; Xia, Y. Z. (2023). Multi-robot path optimization and simulation for multi-route inspection in manufacturing, *International Journal of Simulation Modelling*, Vol. 22, No. 1, 121-132, doi:10.2507/IJSIMM22-1-CO1

[34] Kozłowski, E.; Antosz, K.; Mazurkiewicz, D.; Sęp, J.; Żabiński, T. (2021). Integrating advanced measurement and signal processing for reliability decision-making, *Eksploatacja i Niezawodność – Maintenance and Reliability*, Vol. 23, No. 4, 777-787, doi:10.17531/ein.2021.4.20

[35] Shu, X.; Zhang, S.; Li, Y.; Chen, M. (2022). An anomaly detection method based on random convolutional kernel and isolation forest for equipment state monitoring, *Eksploatacja i Niezawodność – Maintenance and Reliability*, Vol. 24, No. 4, 758-770, doi:10.17531/ein.2022.4.16